

## Systematic investigation of trace anomaly contribution in nucleon mass

Xiao-Yun Wang<sup>1,2,\*</sup> and Jingxuan Bu<sup>1</sup>

<sup>1</sup>Department of Physics, Lanzhou University of Technology, Lanzhou 730050, China

<sup>2</sup>Lanzhou Center for Theoretical Physics, Key Laboratory of Theoretical Physics of Gansu Province, and Key Laboratory of Quantum Theory and Applications of MoE, Lanzhou University, Lanzhou, Gansu 730000, China



(Received 11 February 2024; accepted 7 August 2024; published 21 August 2024)

In this work, under the framework of the vector meson dominance model, the trace anomaly contribution value inside neutrons is extracted for the first time based on vector meson photoproduction data. Furthermore, we systematically compare and analyze the trace anomaly contributions of protons and neutrons. The results show that the trace anomaly contributions of protons and neutrons are close, which indirectly confirms that their internal structures and dynamic properties may have certain similarities. In addition, the main factors affecting the extraction of the trace anomaly contribution of nucleons are discussed in detail. This study not only provides a theoretical basis for us to better understand the source of nucleon mass but also makes a useful exploration and discussion on how to extract the trace anomaly contribution of nucleons more accurately in the future.

DOI: [10.1103/PhysRevC.110.025206](https://doi.org/10.1103/PhysRevC.110.025206)

### I. INTRODUCTION

As the elementary particle of most visible matter, the study on the internal properties of nucleons is a valuable subject of quantum chromodynamics (QCD), where the source of the nucleon mass has always been a mystery. The Higgs mechanism explains only 2% of it, most of the rest come from the complex strong interactions. However, due to the weak gravitational interactions acting on the single nucleon, the source of the nucleon mass cannot be directly measured experimentally. Nevertheless, Ji *et al.* [1–3] found a way to represent the nucleon mass in terms of quark and gluon energy theoretically; the nucleon mass is divided into four parts under their separation.

The separation starts from the QCD energy-momentum tensor (EMT)  $T^{\mu\nu}$ , which can be decomposed into the trace and traceless parts [2]:

$$T^{\mu\nu} = \hat{T}^{\mu\nu} + \bar{T}^{\mu\nu}. \quad (1)$$

Further, the trace part is a sum of the quark mass and trace anomaly contributions, and the traceless part consists of the quark and gluon energy contributions, respectively,

$$\begin{aligned} \hat{T}^{\mu\nu} &= \hat{T}_a^{\mu\nu}(\mu^2) + \hat{T}_m^{\mu\nu}(\mu^2), \\ \bar{T}^{\mu\nu} &= \bar{T}_q^{\mu\nu}(\mu^2) + \bar{T}_g^{\mu\nu}(\mu^2), \end{aligned} \quad (2)$$

and the tensor defines the QCD Hamiltonian operator as [2]

$$H_{\text{QCD}} = \int d^3\vec{x} T^{00}(0, \vec{x}). \quad (3)$$

According to the above definition and decomposition of the EMT, the corresponding four-part separation of the QCD Hamiltonian operator is obtained as [2]

$$H_{\text{QCD}} = H_q + H_g + H_m + H_a. \quad (4)$$

In Ref. [2], the hadron mass is defined as the expectation value of the Hamiltonian operator in the rest frame,

$$M = \frac{\langle P | H_{\text{QCD}} | P \rangle}{\langle P | P \rangle} \Bigg|_{\text{rest frame}}. \quad (5)$$

Thus, based on Eqs. (4) and (5) the hadron mass decomposition is derived as [2]

$$\begin{aligned} M_q &= \frac{3}{4} \left( a - \frac{b}{1 + \gamma_m} \right) M, \\ M_g &= \frac{3}{4} (1 - a) M, \\ M_m &= \frac{4 + \gamma_m}{4(1 + \gamma_m)} b M, \\ M_a &= \frac{1}{4} (1 - b) M. \end{aligned} \quad (6)$$

Noted from the above, the specific values of the mass decomposition are determined by parameters  $a$  and  $b$ , which are the fraction of the nucleon momentum carried by quarks and the trace anomaly parameter, respectively, and  $\gamma_m$  represents the anomalous dimensions [1,2]. Notice that there is a new source of mass that appears in the last term, which is the so-called trace anomaly contribution; it depends only on parameter  $b$ . Ji and Lui [4] argue that the trace anomaly comes

\*Contact author: xywang@lut.edu.cn

Published by the American Physical Society under the terms of the [Creative Commons Attribution 4.0 International](https://creativecommons.org/licenses/by/4.0/) license. Further distribution of this work must maintain attribution to the author(s) and the published article's title, journal citation, and DOI. Funded by SCOAP<sup>3</sup>.

from the scale symmetry breaking among the regulation of the UV divergences, with the scheme being independent. It contributes the nucleon mass by a Higgs-like mechanism and sets the scale of the other parts of the mass separations. Besides, one can carry out the related mechanism of the quark confinement by studying the anomalous energy.

At present, there is some research on the proton trace anomaly contribution, such as the lattice QCD calculation [5] and the holographic calculation [6–8]. However, there are discrepancies in the conclusions between the current works. For instance, in the latest lattice QCD calculation of the proton anomaly contribution, the result is 23% [5]. The predictive ability of the holographic model is presented in Ref. [9] by JLab. They compared the predicted cross section of the holographic model with the experimental data; the results show that the predicted cross section corresponding to the maximum and minimum trace anomaly contributions are very close, which means that the model cannot determine the anomaly contribution at present. In addition, the trace anomaly contribution can also be calculated from the scattering between the quarkonium and the nucleon [6–13]. This implies that we can study the trace anomaly based on the existing photoproduction experimental data by combining the above process with the vector meson photoproduction process under the vector meson dominance (VMD) model [10]. In Ref. [9], the proton trace anomaly contribution is also calculated based on the  $J/\psi$  photoproduction experimental data under the VMD model, but the results show that the anomaly contribution increases obviously with energy. That is, the result calculated at higher energy is larger, which can reach more than 20%; the results extracted near the threshold are very small, only a few percent. In addition, there is also a study about the proton mass decomposition, which starts from the QCD EMT, and after introducing the independent operators, Metz *et al.* [14] concluded that the anomaly contribution of proton is equal to 0. These inconsistent results indicate the necessity of research on the nucleon trace anomaly contribution. In our previous work [12], we modified the VMD model to solve the energy-dependence problem, and the error of the obtained results has been greatly reduced.

There have been some studies on the trace anomaly contribution of protons [5,9,11–13], but not yet on the trace anomaly contribution of neutrons. One of the purposes of this work is to first extract the trace anomaly contribution of the neutron mass under the VMD model. As another purpose, we will further analyze the factors affecting the nucleon anomaly contribution. After Ref. [12], we further extended the work to other vector meson photoproduction processes with an improved method [13], showing that the trace anomaly contributions from different processes are not the same, although they are all relatively small. Such results bring the nucleon anomaly contribution another non-negligible error and inspire us to further analyze the affecting factors in order to give a more accurate proportion of the trace anomaly part. A comprehensive analysis is discussed in detail in Sec. IV, and the research direction of obtaining higher precision nucleon trace anomaly contributions is pointed out. In part before the Summary, the influence of the parameter  $\alpha_s$ , which has a sizable inaccurate precision [15–27], on the nucleon anomaly contribution is

first studied numerically. To achieve this, we adopt two sets of  $\alpha_s$ 's on the extraction named  $\alpha_A$  and  $\alpha_B$ , one set of  $\alpha_s$ 's ( $\alpha_A$ 's) comes from some previous prediction and fitting results [28,29], another group ( $\alpha_B$ ) comes from a recent work [30] on predicting  $\alpha_s$  values based on machine learning methods and large amounts of experimental data.

The structure of the paper is as follows. After the Introduction, a review of the calculation method VMD model is given in Sec. II, the corresponding numerical results are given in Sec. III, and finally a summary is given in Sec. IV.

## II. FORMALISM

In the VMD model, the process  $\gamma N \rightarrow \text{VMN}$  is related with the process  $\text{VMN} \rightarrow \text{VMN}$ , and the forward differential cross section of  $\gamma N \rightarrow \text{VMN}$  reaction is expressed as [10]

$$\left. \frac{d\sigma_{\gamma N \rightarrow \text{VMN}}}{dt} \right|_{t=t_{\min}} = \frac{3\Gamma_{e^+e^-}}{\alpha m_V} \left( \frac{p_{\text{VMN}}}{p_{\gamma N}} \right)^2 \left. \frac{d\sigma_{\text{VMN} \rightarrow \text{VMN}}}{dt} \right|_{t=t_{\min}}, \quad (7)$$

where  $\Gamma_{e^+e^-}$  is the radiative decay width, the value of the electromagnetic coupling constant  $\alpha$  is equal to  $1/137$ , and  $m_V$  is the vector meson mass.  $p_{ab} = \frac{1}{2W} \sqrt{W^4 - 2(m_a^2 + m_b^2)W^2 + (m_a^2 - m_b^2)^2}$  denotes the center-of-mass momentum of the photon and the vector meson, respectively. The differential cross section part of the  $\text{VMN} \rightarrow \text{VMN}$  process in the formula is given as

$$\left. \frac{d\sigma_{\text{VMN} \rightarrow \text{VMN}}}{dt} \right|_{t=t_{\min}} = \frac{1}{64} \frac{1}{m_V^2 (\lambda^2 - M_N^2)} |F_{\text{VMN}}|^2, \quad (8)$$

where the nucleon energy is  $\lambda = (W^2 - m_V^2 - M_N^2)/(2m_V)$  [10], and at the low-energy region, the elastic scattering amplitude of the  $\text{VMN} \rightarrow \text{VMN}$  process is taken as [31]

$$\begin{aligned} F_{\text{VMN}} &\simeq r_0^3 d_2 \frac{2\pi^2}{27} \left( 2M_N^2 - \langle N | \sum_{h=u,d,s} m_h \bar{q}_h q_h | N \rangle \right) \\ &= r_0^3 d_2 \frac{2\pi^2}{27} 2M_N^2 (1 - b), \end{aligned} \quad (9)$$

where the Bohr radius and the Wilson coefficient are [31,32]

$$r_0 = \frac{4}{3\alpha_s m_q}, \quad (10)$$

$$d_n = \left( \frac{32}{N_c} \right)^2 \sqrt{\pi} \frac{\Gamma(n + 5/2)}{\Gamma(n + 5)}, \quad (11)$$

respectively, where  $\alpha_s$  is the strong coupling constant and  $m_q$  is the mass of the constituent quark. The relevant parameters are listed in Table I.

As we can see, the above formula relates the vector meson photoproduction cross section to parameter  $b$ , and the trace anomaly can be represented by  $\frac{1}{4}(1 - b)M$  when away from the chiral limit. Thus, the trace anomaly contribution can be studied through the VMD model. However, the four-momentum transfers  $t_{\min}$  varies significantly with  $W$  while  $t_{\text{thr}} = m_V^2 M_N / (m_V + M_N)$  stays steady [36]. The variation of

TABLE I. The relevant parameters of  $\rho$ ,  $\omega$ , and  $\phi$  [28–30,33–35].

Meson	$\Gamma_{e^+e^-}$ (keV)	$m_q$ (GeV)	$m_V$ (GeV)	$\alpha_A$	$\alpha_B$
$\rho$	7.04	0.330	0.770	0.439	0.601
$\omega$	0.60	0.330	0.782	0.460	0.595
$\phi$	1.27	0.486	1.019	0.770	0.506

$t_{\min}$  leads to an energy dependence of  $\left. \frac{d\sigma_{\gamma N \rightarrow \text{VMN}}}{dt} \right|_{t=t_{\min}}$  that ends up resulting in the energy dependence of the trace anomaly. In Refs. [36,37], the relationship between the differential and total cross sections at the near threshold is given as

$$\begin{aligned} \left. \frac{d\sigma_{\gamma N \rightarrow \text{VMN}}}{dt} \right|_{t=t_{\min}, W=W_{\text{thr}}} &= \left. \frac{d\sigma_{\gamma N \rightarrow \text{VMN}}}{dt} \right|_{t=t_{\text{thr}}, W=W_{\text{thr}}} \\ &= \frac{\sigma_{\gamma N \rightarrow \text{VMN}}(W_{\text{thr}})}{4|p_\gamma| \cdot |p_V|}. \end{aligned} \quad (12)$$

In order to decrease the energy dependence, we would apply the last two methods to study the trace anomaly contribution.

### III. RESULTS AND DISCUSSION

The  $\alpha_A$  values of the three vector mesons come from several previous works, where the  $\alpha_A$  values for  $\omega$  and  $\rho$  are taken from the estimates based on a relativistic-quantum-field model [29], and for  $\phi$ , the  $\alpha_A$  values are taken from the calculations based on a quark potential model [28]. The  $\alpha_B$  values are all derived from the machine learning prediction [30], which varies with the energy scale  $Q$ . Here the respective meson mass is taken as the corresponding energy scale [38].

After determining the relevant parameters, the calculations are carried out. First, based on the experimental differential and total cross sections of  $\omega$  at  $W \in [1.75, 2.15]$  measured by ELSA [39], the neutron trace anomaly contributions were extracted under the framework of the VMD model. Results obtained at  $\alpha_A$  are listed in Table II and shown in Fig. 1

 TABLE II. The neutron trace anomaly contribution extracted from the experimental  $\omega$  photoproduction cross section at  $\alpha_A$  [29,39]. The average is  $1.43^{+0.58}_{-0.33}$  %.

$W$ (GeV)	$M_a/M_N$ (%) (from $d\sigma/dt$ )	$W$ (GeV)	$M_a/M_N$ (%) (from $\sigma$ )
1.76	$1.41 \pm 0.18$	1.76	$1.31 \pm 0.07$
1.78	$1.39 \pm 0.21$	1.78	$1.39 \pm 0.09$
1.79	$1.31 \pm 0.21$	1.79	$1.46 \pm 0.07$
1.81	$1.28 \pm 0.12$	1.81	$1.37 \pm 0.07$
1.84	$1.43 \pm 0.13$	1.84	$1.34 \pm 0.05$
1.86	$1.40 \pm 0.12$	1.86	$1.36 \pm 0.06$
1.90	$1.59 \pm 0.08$	1.90	$1.38 \pm 0.08$
1.95	$1.49 \pm 0.06$	1.95	$1.30 \pm 0.04$
2.00	$1.49 \pm 0.07$	2.00	$1.27 \pm 0.05$
2.04	$1.70 \pm 0.06$	2.04	$1.23 \pm 0.06$
2.09	$1.73 \pm 0.06$	2.09	$1.27 \pm 0.05$
2.13	$1.93 \pm 0.08$	2.13	$1.28 \pm 0.05$

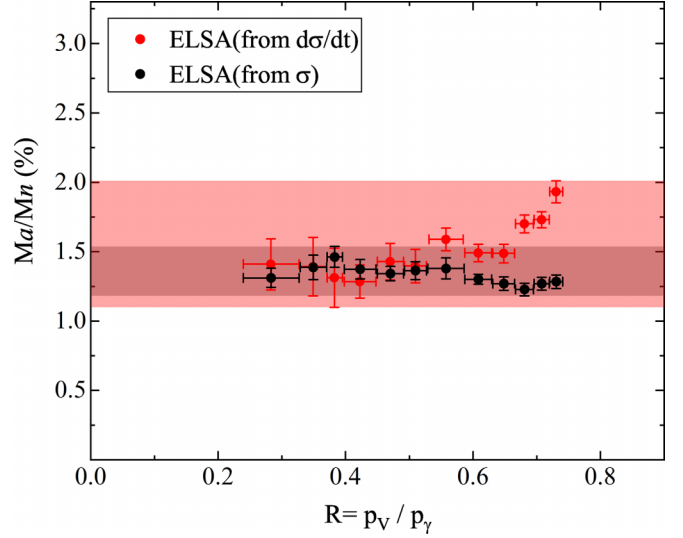


FIG. 1. The neutron trace anomaly contributions  $M_a/M_N$  as a function of  $R$  extracted from the experimental  $\omega$  differential and the total cross section at  $\alpha_A$  [29,39]. The solid red and black circles represent the results from the differential and total cross sections, respectively. Bands in the corresponding color are the error bars.

as a function of  $R$ . The results from the differential and the total cross sections are slightly different due to the numerical difference between the two sections. In order to consider the outcomes in both cases, we process all of the results as a root mean square, (RMS) which is  $1.43^{+0.58}_{-0.33}$  %.

Using the same way of  $\omega$ , the neutron trace anomaly contributions were extracted from the SLAC differential cross section [40] of  $\rho$  photoproduction at  $W = 3.87$  GeV as  $1.50 \pm 0.22$  % under the condition of  $\alpha_A$ . In addition, the neutron trace anomaly contributions are also extracted from the predicted  $\phi$  differential cross section [41] at different energies under  $\alpha_A$ , shown in Table III and Fig. 2 as a function of  $R$ , and the root mean square of the results is  $7.89^{+1.74}_{-4.61}$  %. However, the results from the  $\phi$  photoproduction process vary greatly under different energies, which is caused by the uncertainty of the prediction. So this set of results is for reference only.

Under the VMD model, the trace anomaly contribution of the neutron has been extracted, where  $\alpha_s$  values are derived from several different physical models. Another purpose is to discuss the effect of  $\alpha_s$  variation on the anomaly contribution. We extract the anomaly contribution at  $\alpha_B$  with the same method through three vector meson photoproduction processes;  $\alpha_B$  comes from the pure prediction by data learning and has no model dependence [30]. The trace anomaly contribution RMS of the neutron mass at different  $\alpha_s$  values are

 TABLE III. The neutron trace anomaly contributions extracted from the predicted  $\phi$  photoproduction differential cross section at  $\alpha_A$  [28,41]. The average is  $7.89^{+1.74}_{-4.61}$  %.

$W$ (GeV)	2.01	2.12	2.15
$M_a/M_N$ (%)	9.12	9.63	3.27

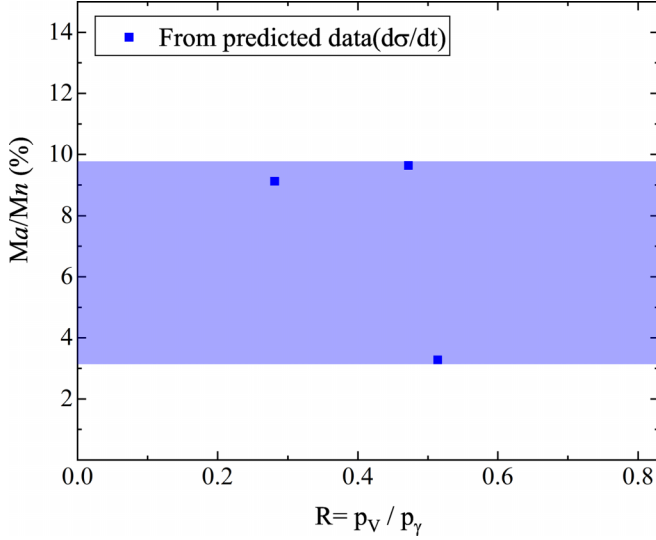


FIG. 2. The neutron trace anomaly contributions from the predicted  $\phi$  differential cross section at  $\alpha_A$  as a function of  $R$  [28,41], which are represented by the solid blue squares. The blue band is the error bar.

compared in Table IV. Combined with the value of  $\alpha_s$  shown in Table I, one finds that the trace anomaly contribution is very sensitive to it. That indicates  $\alpha_s$  is a crucial uncertain physical quantity for itself and for calculating the nucleon anomaly contribution.

In Refs. [12] and [13], the trace anomaly contributions of the proton mass were extracted through the heavy and light vector meson photoproduction processes. We display the comparison of the proton and neutron results at the same set of  $\alpha_s$  ( $\alpha_A$ ) values in Table V. The results indicate that the trace anomaly contributions between neutrons and protons from the same photoproduction are close considering the error bar, although the results from the different processes are still different from each other.

As for the percentage of the nucleon anomaly contribution, although the results obtained with the present calculation accuracy from our works show that it is small, it cannot be taken as the final conclusion yet; the specific reasons for this are discussed in the next section.

#### IV. SUMMARY

In this work, we calculated the trace anomaly contribution of the neutron mass through the light vector meson photoproduction processes for the first time based on the VMD model.

TABLE IV. The trace anomaly contribution RMS of the neutron at two sets of  $\alpha_s$  [28–30].

Meson	$\rho$	$\omega$	$\phi$
$M_a/M_N$ (%) (from $\alpha_A$ )	$1.50 \pm 0.22$	$1.43^{+0.58}_{-0.33}$	$7.89^{+1.74}_{-4.61}$
$M_a/M_N$ (%) (from $\alpha_B$ )	$3.85 \pm 0.56$	$3.10^{+1.26}_{-0.72}$	$2.24^{+0.50}_{-1.31}$

TABLE V. The trace anomaly contribution RMS of nucleons at  $\alpha_A$  [13,28,29].

Meson	$\rho$	$\omega$	$\phi$
$M_a/M_N$ (%) (proton)	$0.53 \pm 0.15$	$1.47 \pm 0.48$	$3.63 \pm 0.64$
$M_a/M_N$ (%) (neutron)	$1.50 \pm 0.22$	$1.43^{+0.58}_{-0.33}$	$7.89^{+1.74}_{-4.61}$

The numerical results obtained from the three processes are all relatively small:  $1.43^{+0.58}_{-0.33}$  % from the  $\omega$  photoproduction,  $1.50 \pm 0.22$  % from the  $\rho$  photoproduction, and  $7.89^{+1.74}_{-4.61}$  % from the  $\phi$  photoproduction. At the same time, the results show that under the same parameter the trace anomaly contributions of protons and neutrons are very close, indicating that the mass distribution and quark-gluon structure inside them may be similar. We also studied the influence of parameter  $\alpha_s$  on the nucleon anomaly contribution and proved that  $\alpha_s$  has a significant effect on it. In addition, the accuracy of the experimental data of photoproduction cross sections and the differences of vector meson production mechanisms also affect the extraction of the trace anomaly contribution of nucleons.

In terms of experimental data, the current shortcoming is that the neutron-target photoproduction data are insufficient. However, the proton-target photoproduction data are relatively abundant, we consider that there is a possibility of using machine learning algorithms to predict the cross section of the  $J/\psi$  photoproduction of neutrons. Besides, the physical model could be effective in predicting the neutron-target photoproduction data due to the exclusive reaction channels of the  $J/\psi$  production. We will explore the above aspects in our follow-up work. At the same time, more high-precision experimental measurements for the photoproduction are expected.

As for the differences in vector meson production mechanisms, we found that the difference in mesons' related properties visibly affects the nucleon trace anomaly contribution by analyzing the results from different photoproduction processes under the VMD model. For example, the decay width of mesons has a significant effect on the proton anomaly contribution. The  $\omega$  meson and the  $\rho$  meson have a similar mass, corresponding  $\alpha_s$ , and component quark mass, but there is a large gap between the anomaly contribution results calculated from the two processes, which comes from the large decay width of  $\rho$ . These results bring the anomaly contribution of the proton mass a notable error; if the partial width  $\Gamma_{\rho \rightarrow e^+e^-}$  of  $\rho$  is set as  $\Gamma_{\omega \rightarrow e^+e^-}$ , the results of the proton anomaly contribution will be very close [13]. Based on the verification in Sec. III, we have learned that  $\alpha_s$  is an important parameter, noticeably affecting the nucleon trace anomaly contribution. At the same time,  $\alpha_s$  also has a large uncertainty in the low-energy range, this is due to the complexity of the nonperturbative QCD. Meanwhile, the corresponding scales of  $\alpha_s$ , which are taken as the meson mass, are included within this range exactly. The appreciable error of  $\alpha_s$  and its significant effect on the nucleon trace anomaly contribution leads to the uncertainty of the anomaly contribution.

We continue using the machine learning algorithms to study  $\alpha_s$ , to explore the physics involved and try to correct its accuracy. In fact,  $\alpha_s$  has great accuracy both experimentally and theoretically in the high- $Q$  range. If photoproduction experimental data of heavier mesons are available, the uncertainty from  $\alpha_s$  will be eliminated through the calculations from these processes.

The scattering length of VMN can also be calculated under the VMD model, and the related studies are abundant [36,37,42–45]. Meanwhile, the uncertainty of the involved parameters in the calculation is small. Therefore, we will consider exploring the possibility of associating the VMN scattering length with the nucleon trace anomaly contribution under the VMD model, trying to find another way to reveal the nucleon trace anomaly contribution.

In conclusion, although the current numerical results of the nucleon trace anomaly contribution are small, this can only be considered a partial conclusion due to a series of uncertainties. We will conduct our follow-up based on the above points, aiming to extract a more accurate nucleon trace anomaly contribution.

## ACKNOWLEDGMENTS

This work is supported by the National Natural Science Foundation of China under Grants No. 12065014 and No. 12247101 and by the Natural Science Foundation of Gansu Province under Grant No. 22JR5RA266. We acknowledge the West Light Foundation of The Chinese Academy of Sciences, Grant No. 21JR7RA201.

- 
- [1] X. D. Ji, A QCD analysis of the mass structure of the nucleon, *Phys. Rev. Lett.* **74**, 1071 (1995).
- [2] X. D. Ji, Breakup of hadron masses and energy-momentum tensor of QCD, *Phys. Rev. D* **52**, 271 (1995).
- [3] C. Lorcé, On the hadron mass decomposition, *Eur. Phys. J. C* **78**, 120 (2018).
- [4] X. Ji and Y. Liu, Quantum anomalous energy effects on the nucleon mass, *Sci. China Phys. Mech. Astron.* **64**, 281012 (2021).
- [5] F. He, P. Sun, and Y. B. Yang ( $\chi$ QCD Collaboration), Demonstration of the hadron mass origin from the QCD trace anomaly, *Phys. Rev. D* **104**, 074507 (2021).
- [6] Y. Hatta, A. Rajan, and K. Tanaka, Quark and gluon contributions to the QCD trace anomaly, *J. High Energy Phys.* **02** (2018) 008.
- [7] Y. Hatta, A. Rajan and D. L. Yang, Near threshold  $J/\psi$  and  $\Upsilon$  photoproduction at JLab and RHIC, *Phys. Rev. D* **100**, 014032 (2019).
- [8] Y. Hatta and D. L. Yang, Holographic  $J/\psi$  production near threshold and the proton mass problem, *Phys. Rev. D* **98**, 074003 (2018).
- [9] B. Duran, Z. E. Meiziani, S. Joosten, M. K. Jones, S. Prasad, C. Peng, W. Armstrong, H. Atac, E. Chudakov, H. Bhatt *et al.*, Determining the gluonic gravitational form factors of the proton, *Nature (London)* **615**, 813 (2023).
- [10] D. Kharzeev, H. Satz, A. Syamtomov, and G. Zinovjev,  $J/\psi$  Photoproduction and the gluon structure of the nucleon, *Eur. Phys. J. C* **9**, 459 (1999).
- [11] R. Wang, J. Evslin, and X. Chen, The origin of proton mass from  $J/\psi$  photo-production data, *Eur. Phys. J. C* **80**, 507 (2020).
- [12] X. Y. Wang, J. Bu, and F. Zeng, Analysis of the contribution of the quantum anomaly energy to the proton mass, *Phys. Rev. D* **106**, 094029 (2022).
- [13] C. Dong, J. Zhang, J. Bu, H. Zhou, and X. Y. Wang, Exploration of trace anomaly contribution to proton mass based on light vector meson photoproduction, *Eur. Phys. J. C* **83**, 122 (2023).
- [14] A. Metz, B. Pasquini, and S. Rodini, Revisiting the proton mass decomposition, *Phys. Rev. D* **102**, 114042 (2020).
- [15] A. Deur, S. J. Brodsky, and G. F. de Teramond, The QCD running coupling, *Prog. Part. Nucl. Phys.* **90**, 1 (2016).
- [16] S. Narison, QCD parameter correlations from heavy quarkonia, *Int. J. Mod. Phys. A* **33**, 1850045 (2018).
- [17] E. Braaten, S. Narison, and A. Pich, QCD analysis of the tau hadronic width, *Nucl. Phys. B* **373**, 581 (1992).
- [18] A. Deur, V. Burkert, J. P. Chen, and W. Korsch, Experimental determination of the effective strong coupling constant, *Phys. Lett. B* **650**, 244 (2007).
- [19] A. Deur, V. Burkert, J. P. Chen, and W. Korsch, Determination of the effective strong coupling constant  $\alpha_{s,g_1}(Q^2)$  from CLAS spin structure function data, *Phys. Lett. B* **665**, 349 (2008).
- [20] A. Deur, V. Burkert, J. P. Chen, and W. Korsch, Experimental determination of the QCD effective charge  $\alpha_{g_1}(Q)$ , *Particles* **5**, 171 (2022).
- [21] A. Deur, J. P. Chen, S. E. Kuhn, C. Peng, M. Ripani, V. Sulkosky, K. Adhikari, M. Battaglieri, V. D. Burkert, G. D. Cates *et al.* Experimental study of the behavior of the Bjorken sum at very low  $Q^2$ , *Phys. Lett. B* **825**, 136878 (2022).
- [22] K. Ackerstaff *et al.* (HERMES Collaboration), Measurement of the neutron spin structure function  $g_1^n$  with a polarized  $^3\text{He}$  internal target, *Phys. Lett. B* **404**, 383 (1997).
- [23] K. Ackerstaff *et al.* (HERMES Collaboration), Determination of the deep inelastic contribution to the generalized Gerasimov-Drell-Hearn integral for the proton and neutron, *Phys. Lett. B* **444**, 531 (1998).
- [24] A. Airapetian *et al.* (HERMES Collaboration), Measurement of the proton spin structure function  $g_1^p$  with a pure hydrogen target, *Phys. Lett. B* **442**, 484 (1998).
- [25] A. Airapetian *et al.* (HERMES Collaboration), Evidence for quark hadron duality in the proton spin asymmetry  $A_1$ , *Phys. Rev. Lett.* **90**, 092002 (2003).
- [26] A. Airapetian *et al.* (HERMES Collaboration), Precise determination of the spin structure function  $g_1$  of the proton, deuteron and neutron, *Phys. Rev. D* **75**, 012007 (2007).
- [27] Q. Yu, H. Zhou, X. D. Huang, J. M. Shen, and X. G. Wu, Novel and self-consistency analysis of the QCD running coupling  $\alpha_s(Q)$  in both the perturbative and nonperturbative domains, *Chin. Phys. Lett.* **39**, 071201 (2022).
- [28] M. S. Liu, K. L. Wang, Q. F. Lü, and X. H. Zhong,  $\Omega$  baryon spectrum and their decays in a constituent quark model, *Phys. Rev. D* **101**, 016002 (2020).
- [29] G. Ganbold, QCD effective coupling in the infrared region, *Phys. Rev. D* **81**, 094008 (2010).
- [30] X. Y. Wang, C. Dong, and X. Liu, Machine learning the governing principle of strong coupling constant across the global energy scale, *Chin. Phys. Lett.* **41**, 031201 (2023).

- [31] D. Kharzeev, Quarkonium interactions in QCD, in *Selected Topics in Non-Perturbative QCD, Proceedings of the International School of Physics "Enrico Fermi,"* Course CXXX, Varenna, Italy, June 1995, edited by A. Di Giacomo and D. Diakonov (IOS, Amsterdam, 1996), pp. 105–131.
- [32] D. Kharzeev, H. Satz, A. Syamtomov, and G. Zinovev, On the sum rule approach to quarkonium-hadron interactions, *Phys. Lett. B* **389**, 595 (1996).
- [33] R. L. Workman *et al.* (Particle Data Group), Review of particle physics, *Prog. Theor. Exp. Phys.* **2022**, 083C01 (2022).
- [34] Q. Zhao, Z. P. Li, and C. Bennhold,  $\omega$  and  $\rho$  photoproduction with an effective quark model Lagrangian, *Phys. Lett. B* **436**, 42 (1998).
- [35] W. Kou, R. Wang, and X. Chen, Extraction of proton trace anomaly energy from near-threshold  $\phi$  and  $J/\psi$  photoproductions, *Eur. Phys. J. A* **58**, 155 (2022).
- [36] L. Pentchev and I. I. Strakovsky,  $J/\psi$ - $p$  scattering length from the total and differential photoproduction cross sections, *Eur. Phys. J. A* **57**, 56 (2021).
- [37] A. I. Titov, T. Nakano, S. Date, and Y. Ohashi, Comments on differential cross-section of  $\phi$ -meson photoproduction at threshold, *Phys. Rev. C* **76**, 048202 (2007).
- [38] N. Brambilla, X. Garcia-Tormo, J. Soto, and A. Vairo, Extraction of  $\alpha_s$  from radiative  $\Upsilon(1S)$  decays, *Phys. Rev. D* **75**, 074014 (2007).
- [39] F. Dietz *et al.* (CBELSA/TAPS Collaboration), Photoproduction of  $\omega$  mesons off protons and neutrons, *Eur. Phys. J. A* **51**, 6 (2015).
- [40] G. Alexander, J. Gandsman, A. Levy, D. Lissauer, and L. M. Rosenstein, Study of  $\rho^0$  production in  $\gamma d$ ,  $\gamma p$  and  $\gamma n$  reactions at 7.5 GeV using linearly polarized photon beam, *Nucl. Phys. B* **69**, 445 (1974).
- [41] Q. Zhao, Study  $\omega$  and  $\phi$  photoproduction in the nucleon isotopic channels, in *Proceedings of the International Symposium on Electromagnetic Interactions in Nuclear and Hadron Physics*, edited by M. Fujiwara and T. Shima (World Scientific, Singapore, 2002).
- [42] X. Y. Wang, F. Zeng, and I. I. Strakovsky,  $\psi^{(*)}p$  scattering length based on near-threshold charmonium photoproduction, *Phys. Rev. C* **106**, 015202 (2022).
- [43] X. Y. Wang, F. Zeng, Q. Wang, and L. Zhang, First extraction of the proton mass radius and scattering length  $|\alpha_{\rho^0 p}|$  from  $\rho^0$  photoproduction, *Sci. China Phys. Mech. Astron.* **66**, 232012 (2023).
- [44] X.-Y. Wang, C. Dong, and Q. Wang, Analysis of the interaction between  $\phi$  meson and nucleus, *Chin. Phys. C* **47**, 014106 (2023).
- [45] I. I. Strakovsky, L. Pentchev, and A. I. Titov, Comparative analysis of  $\omega p$ ,  $\phi p$ , and  $J/\psi p$  scattering lengths from A2, CLAS, and GlueX threshold measurements, *Phys. Rev. C* **101**, 045201 (2020).